THE SLAC LINEAR COLLIDER AND A FEW IDEAS ON FUTURE LINEAR COLLIDERS*

GREGORY A. LOEW
Stanford Linear Accelerator Center
Stanford University, Stanford, California 94305

Introduction

This paper comes in two parts. The first part is a progress report on the SLAC Linear Collider (SLC) with emphasis on those systems which are of special interest to linear accelerator designers; it sets the stage for a number of contributed papers on specific topics which are also presented at this conference. The second part presents some ideas which are of interest to the design of future linear colliders of higher energies.

Progress Report on the SLAC Linear Collider

The SLAC Linear Collider (SLC) which has already been described in a number of publications,[1,2,3] is now under construction. The principal SLC parameters at the e^+e^- interaction point are given in table 1 and the overall statistics and milestones of the project as they are seen at this time are given in table 2.

Table 1. SLC Design Parameters at Interaction Point

Number of $e^{\pm}$/bunch	5×10^{10}
Center-of-mass energy	50 on 50 GeV
Luminosity excluding pinch effect	2.1×10^{30}
Luminosity including pinch effect	6×10^{30}
Beam transverse dimensions ($\sigma_x = \sigma_y$)	1.3 micron
Invariant emittance ($\gamma\sigma_x\sigma'_x = \gamma\sigma_y\sigma'_y$)	3×10^{-5} rad-m
$\Delta p/p$	1%
Bunch length (σ_z)	1 mm
Repetition rate	180 pps

Table 2. SLC Budget and Key Dates

Total construction cost	$113 M
Construction period	Oct. 1983 – Sept. 1986
Beginning of overall commissioning	Oct. 1986
First operation of SLC Injector	Spring 1981
Commissioning of first Damping Ring	Early 1983
First nine-sector tests	Jan. 1984
Completion of arc tunnels to date	1/3
Break-in into linac and beam switchyard	Summer 1984

Figure 1 is a schematic representation of the overall SLC layout. As can be seen by comparison with earlier publications, this layout has not changed very much since the original proposal, except that the two damping rings are now to be located in separate vaults with mirror symmetry with respect to the axis of the accelerator. This recent change was made for ease of installation and testing. Figure 2 shows a photograph of the overall SLAC site in which the dotted lines indicate the location of the SLC arcs. The building for the final interaction point has been sketched in.

Linac Improvements

In order to meet the SLC specifications, a gradual linac improvement program has been underway since 1981. This improvement program includes a new injector (Collider Injector Development or CID), a new focusing system and beam

*Work supported by the Department of Energy, contract DE-AC03-76SF00515.

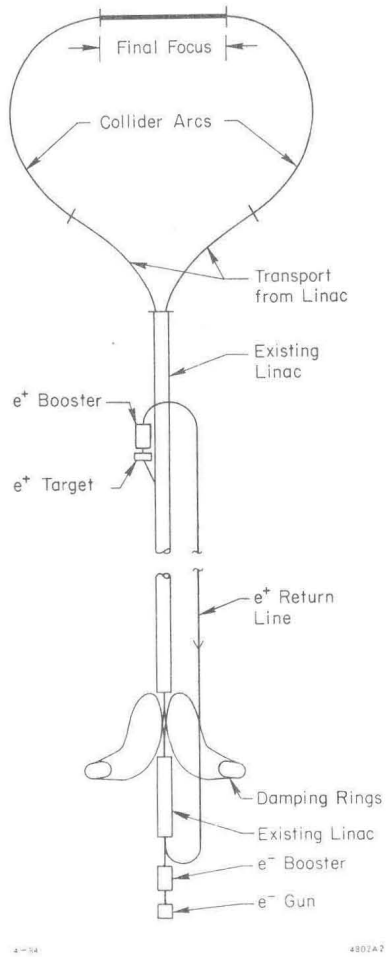

Fig. 1. Overall SLC layout.

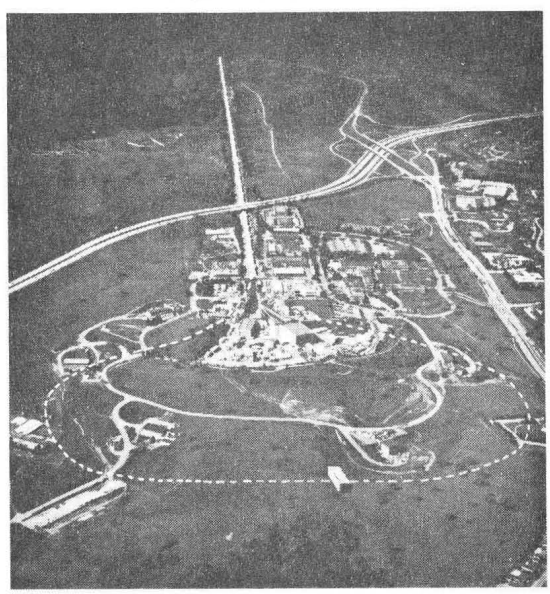

Fig. 2. SLAC site indicating the location of the SLC arcs.

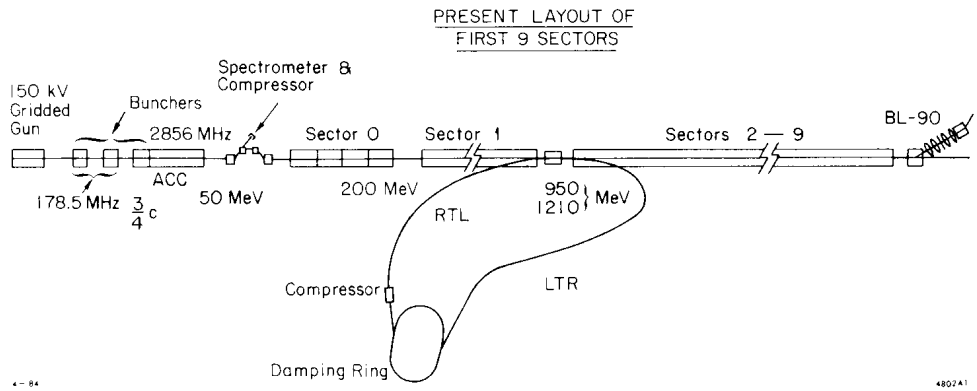

Fig. 3. Present layout of first nine sectors.

position monitors, an improved rf system and an entirely new instrumentation and control system. In January 1984, the first nine sectors of the linac were tested under these new conditions with SLC-type beams, in conjunction with the first damping ring and compressor. A special spectrometer and beam diagnostic station called Beamline 90 was inserted at the beginning of Sector 10. A schematic of the entire layout is shown in fig. 3.

Table 3. SLC Injector (CID)

	Achieved	Final Design
Energy (MeV)	50	50
Electrons/bunch (10^{10})	5 15	≥ 5
Emittance (rad-m $\times 10^{-5}$)		
$\gamma\sigma_x\sigma'_x = \gamma\sigma_y\sigma'_y$	15	30
Bunch length σ_z (mm)		
Uncompressed	2.5	~ 2
Compressed	1.9	
$\Delta p/p$		
Uncompressed	1%	2%
Compressed	10%	
Number of bunches	1	2
Bunch spacing (nsec)		58.82

Details on the injector design and performance can be found in ref. 4 and in a paper presented by J. E. Clendenin *et al.*, at this conference.[5] The principal beam parameters for the injector are summarized in table 3, above. The first column indicates the results achieved so far and the second column gives the final design requirements. As can be seen, the CID injector, which operates with a thermionic gun, has already met most of these final requirements, except that so far it has only produced one bunch rather than two. The second bunch is needed to produce the positrons and it is supposed to trail the first bunch by 17.634 m (58.82 nsec) which corresponds to half the circumference of the damping ring. At the present time the frequency of the subharmonic buncher (178.5 MHz) is not compatible with this bunch spacing. It is likely that in the next eighteen months the two identical subharmonic bunchers will be replaced by two different ones, the first one probably operating at 119 MHz and the second one at 714 MHz. It is expected that this modification will give higher charge, superior bunching and possibly make unnecessary the use of the compressor which follows the first accelerator section. Development of the laser driven photocathode gun is also under progress but will not be installed on the linac for some time.

Table 4 gives the parameters for Sectors 0 and 1 which prepare the beam for injection into the damping ring. Most of the results achieved so far were obtained at 950 MeV (Non SLED). Toward the end of the recent operating period, the linac was run under dedicated SLC conditions and the energy was successfully increased to the final design value of 1210 MeV (SLED I). Note that the maximum number of electrons delivered per bunch to the end of Sector 1 was 1.75×10^{10} which falls short by a factor of 3 of the final design. A much stronger focusing system consisting of new quadrupoles (20.3 cm long and 11.5 cm bore) which will be wrapped around the accelerator structure and spaced so as to keep a constant envelope at constant field (1.5 T-m/m), will be installed during the coming months in Sectors 0 and 1. It should greatly ease the transmission of the high current electron bunches as well as provide the ultimate phase space acceptance of the positron bunches returning from the e^+ source in Sector 19.

Table 4. Sector 0 and 1 Parameters (e^-)

	Achieved		Final Design
Energy (MeV)	950 (Non SLED)	1210 (SLED I)	1210
Electrons/bunch	1.75×10^{10}		5×10^{10}
Emittance (rad-m $\times 10^{-5}$)	Not measured recently		
$\gamma\sigma_x\sigma'_x = \gamma\sigma_y\sigma'_y$			30
$\Delta p/p$	$\leq 1\%$		$\leq 2\%$
Number of bunches	$1\ e^-$	$1\ e^-$	$2e^-$ *
FODO array	Old QA Quads		New Wrap-around Quads
Maximum gradient-length (T-m/m)	1.2		1.5
Quad-spacing (m)	12.34		Linear taper with energy to give constant beam envelope
Betatron phase-shift/cell	72°		Tapered (40° avg.)
β_{max} (m)	41.2		$1.5 < \beta_{max} < 13$
β_{min} (m)	10.7		$0.5 < \beta_{min} < 5$

* ($+1e^+$ in Sec. 1)

The results of the first nine sector tests and a description of the new equipment that was used are given in a paper presented by J. C. Sheppard *et al.*, at this conference.[6] As reported in that paper, these tests were performed by injecting the beam from Sector 1 into the LTR line (see fig. 3) and the south damping ring, damping the bunches during a linac interpulse period of selectable duration, and then re-ejecting the single bunches into the compressor, the RTL line and the linac at the beginning of Sector 2. The goal of transmitting single bunches of 10^{10} electrons at 6.5 GeV to the end of Sector 9 within an invariant emittance ($\gamma\sigma\sigma'$) of approximately 3×10^{-5} rad-m and a $\Delta p/p < 1\%$ was achieved.

Positron Source

The positron source[7] will be located at the end of Sector 19. A schematic of the layout is shown in fig. 4. A pulse magnet on axis of the accelerator will deflect the second electron bunch, extract it from the linac and direct it onto the target. The positron source parameters are shown in table 5. Directly following the slowly rotating target, there will be a pulsed flux concentrator with an initial axial field of 80 kG. This concentrator will be followed by a DC 5-kG solenoid wrapped around the accelerator sections. The accelerator itself will probably consist of two parts, the first being a one-meter 70 MV/m section, and the second one consisting of four three-meter sections at 20 MV/m. It is hoped that with this design,[8] a yield of three positrons per incident electron will be obtained within the desired emittance, thereby giving ample reserve for possible positron losses in the return line, Sector 1 and the e^+ damping ring.

Energy Upgrade to 50 GeV

To achieve an energy of 50 on 50 GeV at the interaction point, the linac must be capable of producing up to 55 GeV because 3 to 4 GeV will be lost by locating the bunches ahead of the rf crest to compensate for beam loading, and 1 GeV will be lost in the SLC arcs by synchrotron radiation. This results in a required energy contribution of $\sim$ 250 MeV/klystron. To achieve this requirement, we will use 50 MW klystrons in conjunction with the SLED scheme[9] operating with 5 μsec pulses (SLED II). Work on the 50 MW klystron has progressed to the point where prototypes have now been operated successfully in the laboratory, except for some unsolved problems with the windows. The klystrons and modulator specifications are summarized in table 6. More details on the klystrons can be found in a paper by G. T. Konrad[10], also presented at this conference.

Table 5. Positron Source Parameters

Incident e^- beam	
Energy (GeV)	33
e^-/bunch	5×10^{10}
σ_x, σ_y (mm)	0.6
Pulse energy (joules)	264
Power at 180 pps (kW)	47
Target (rotating)	
Material	90% Ta – 10% W
Length (mm)	24 (6 rad. lengths)
Rate of rotation	2 Hz
Energy deposition/pulse (joules)	53
Steady-state $T°$ (C)	200
Peak $T°$ (C)	580
Stress (psi)	32000
e^+ beam	
$(\frac{e^+}{e^-})$ yield within 18 mm aperture, 2-20 MeV, $\leq 15°$	~ 3
Invariant emittance (rad-m $\times 10^{-5}$)	1000
Transverse emittance at target	2 mm $\times 2.5 \frac{MeV}{c}$
Initial flux concentrator field (kG)	80
Transverse emittance into 5 kG solenoid	8 mm $\times 0.6 \frac{MeV}{c}$
Gradient in first meter of acceleration ($\frac{MV}{m}$)	70
Gradient in next 12 meters of acceleration ($\frac{MV}{m}$)	20

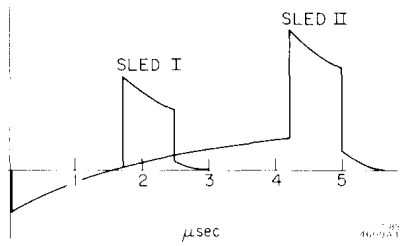

	I	II
Pulse length	2.7 μsec	5 μsec
Energy gain ($e^{\pm}$)	1.40	1.77
Maximum repetition rate	360 pps	180 pps
Klystron power	34 MW	50 MW
Energy per klystron	163 MeV	**250 MeV**

Fig. 5. SLED options with klystron power upgrade.

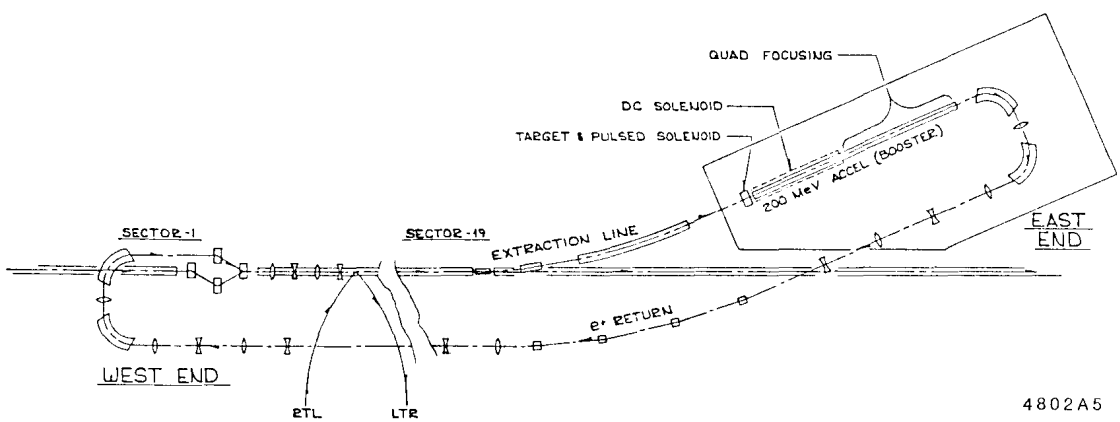

Fig. 4. Schematic of positron source at Sector 19 and return line to Sector 1.

The rf pulses produced by the SLED cavities and the maximum energies that can be obtained as the incident klystron pulse is increased from 2.7 μsec (SLED I) to 5 μsec (SLED II) are illustrated in fig. 5. The SLED II energy vs. time is shown in fig. 6.

Table 6. Klystron-Modulator Specifications

Klystron peak output power	36 MW	50 MW
Frequency	2856 MHz	2856 MHz
Perveance	2.1×10^{-6}	2×10^{-6}
Peak beam voltage	265 KV	315 KV
Peak beam current	286 A	354 A
Peak beam power	75.8 MW	111.5 MW
Average beam power	91.5 kW	120.3 kW
Klystron impedance	926 Ω	890 Ω
Nominal rf pulse width	2.5 μsec	5 μsec
Modulator pulse width	3.35 μsec	6 μsec
Repetition rate	360 pps	180 pps
Klystron efficiency	0.47	0.45
Pulse transformer ratio	1:12	1:14
PFN impedance	6 Ω	4.6 Ω
DC power	107.6 kW	141.6 kW
AC power	119.5 kVA	157 kVA
Focusing magnet	Permanent	Electromagnet
Cathode type	Oxide	Dispenser

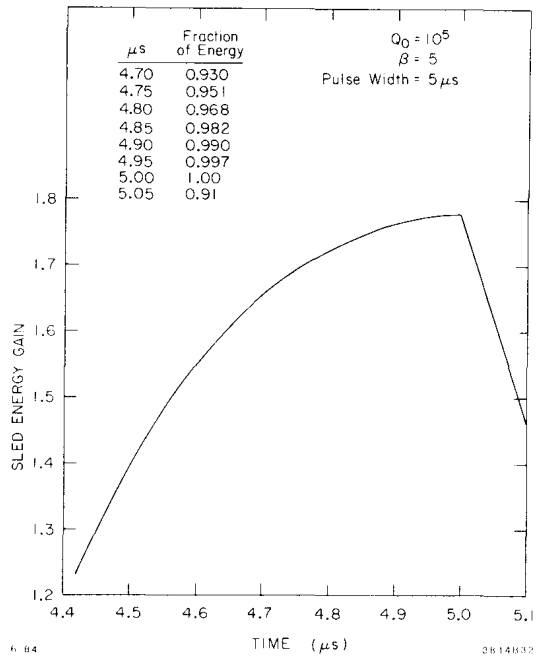

Fig. 6. SLED II gain versus time.

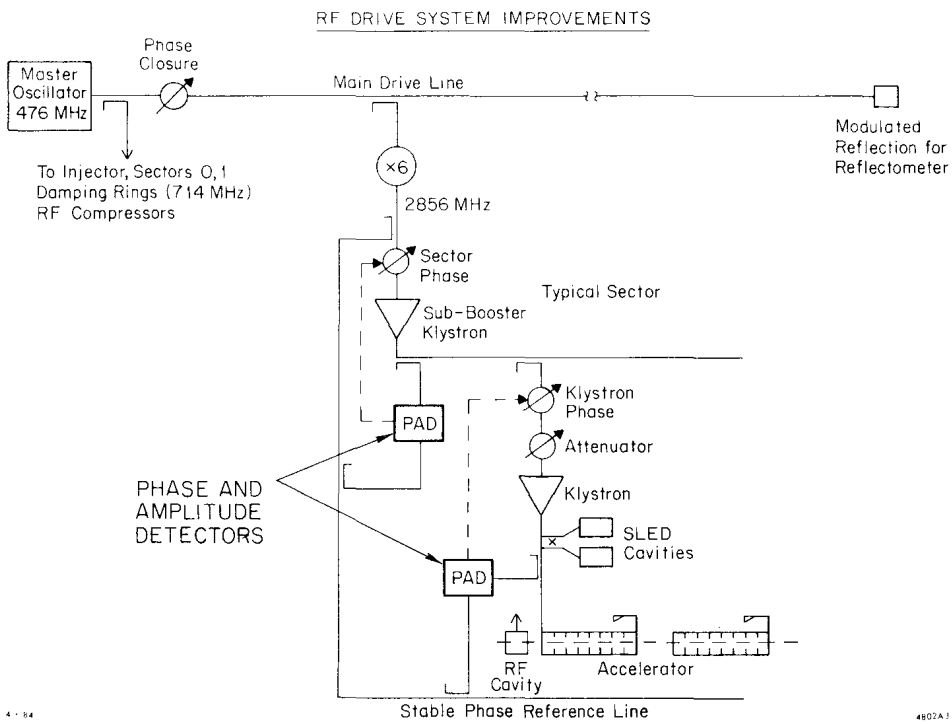

Fig. 7. rf Drive system improvements.

rf Drive System Improvements

For the linac to meet the SLC specifications on energy stability and control of transverse emittance, the entire rf drive system and klystron control have to be improved. Several of the improvements being implemented are shown in fig. 7. These include a major upgrade in the master oscillator system at 476 MHz which feeds the main drive line, a reflectometer at the end of this main drive line to measure its overall phase stability, and in each sector, phase and amplitude detectors (PADs)[11] to monitor an entire sector as well as individual klystrons.

An extra temperature-stabilized reference line has been installed along each sector to provide stable signals against which the individual klystron signals can be compared. Ultimately, these PADs will be used not only to monitor phase and amplitude but also to effect local automatic feedback loops. Sample amplitude and phase measurements obtained with these PADs are shown in figs. 8a and 8b.

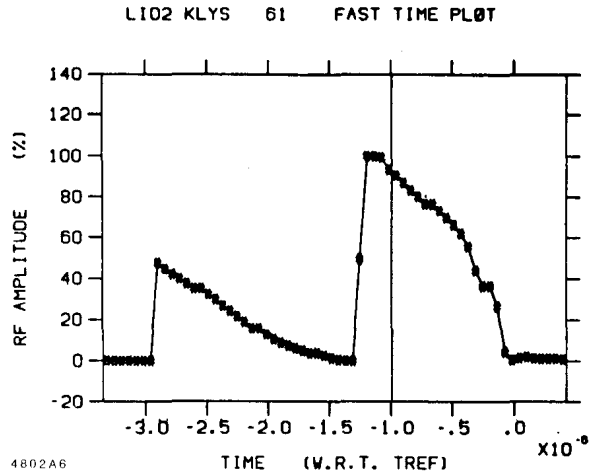

Fig. 8a. Example of rf amplitude measurement made on 36 MW klystron (SLED I).

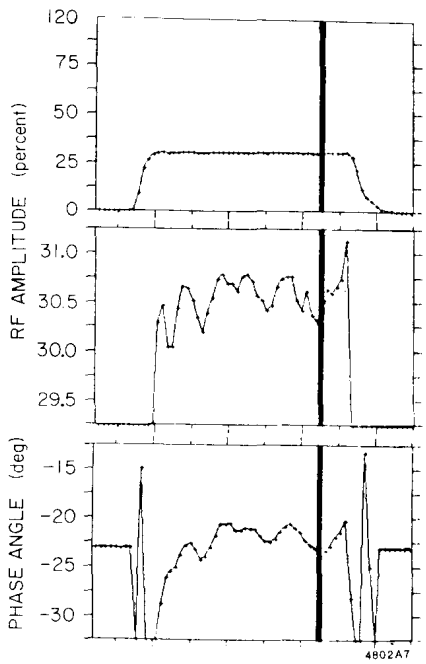

Fig. 8b. Examples of rf amplitude and phase measurements made on 36 MW klystron (Non SLED).

SLC Arcs, Final Focus and Overall I&C

In addition to the topics covered above, there is of course a large effort on design, testing and construction devoted to the SLC arcs, the final focus and the detectors. Although these systems are of crucial importance to the SLC project, they are left out of this report because of lack of space and because they are not be of direct interest to linear accelerator designers. The I&C system for the SLC is partially covered in a paper by M. Crowley-Milling[12], also presented at this conference. A more complete summary can be found in ref. 13.

A Few Ideas on Future Linear Colliders

In looking at the next generation of $e^{\pm}$ colliders in the post-SLC era, a study group at SLAC is focusing on the design of a linear collider system with a center-of-mass energy of 2 TeV and a luminosity of 10^{33} cm^{-2} sec^{-1}. An endeavor of this magnitude is of course a very complex one which encompasses the study of many fundamental questions, such as:

1. What are the ultimate lower limits on emittances obtainable with single bunches or trains of bunches?
2. What are the specifications on the damping rings which presumably are necessary to produce these bunches for injection into the linacs?
3. Since emittance growth along the linacs is due in large part to transverse wake fields, what are the accelerating structure wake field, alignment and focusing requirements on such linacs?
4. Can bunches with sub-micron transverse dimensions be obtained in the final focus?
5. If so, what are the allowable limits on energy spread due to the synchrotron radiation or "beamstrahlung" produced by the magnetic field of one bunch on the other?

Comprehensive answers to these questions are not yet available and their study is beyond the scope of this report. There are, however, three other questions on which some interesting work has recently been done at SLAC and which will be summarized here.

The first question has to do with the rf energy required to build such a machine. A detailed study of such requirements can be found in ref. 14. For this discussion, however, consider the simple expression for the r/Q per unit length of an accelerating structure where r is the shunt impedance/unit length and Q is the usual loss factor:

$$\frac{r}{Q} = \frac{E^2}{\omega W} \qquad (1)$$

where E is the accelerating gradient and W is the energy stored per unit length. For a linac of length L and energy V, the total energy stored is

$$WL = \frac{EV}{\omega \frac{r}{Q}} \quad . \qquad (2)$$

This result is independent of how the energy is deposited in the structure where the beam interacts with it. What eq. (2) shows is that for a given desired energy V, the energy stored scales directly with the gradient and inversely with the square of the frequency because r/Q scales directly with frequency. To illustrate the consequences of these observations, examples of three different 1 TeV linacs have been tabulated in table 7, next to the actual SLC numbers. The SLC conversion efficiency of 6.5% is low because the SLED scheme is inherently inefficient. The assumed conversion efficiency of 25% for the 1 TeV cases is optimistic but is taken to fix our ideas on actual power consumptions. It is seen that at 2856 MHz, the AC powers required are large and the incentive to go to higher frequencies is very strong, particularly since the final numbers must be

doubled because two linacs (e^+ and e^-) are needed. This advantage must be weighed against the disadvantage that the transverse wake field amplitude scales inversely with the fourth power of the beam aperture in the structure, and that high power rf sources may be harder to obtain at higher frequencies. Also, since it is probably not practical to extract much more than 20% of the stored energy with the beam, the remaining 80% of the energy will be wasted unless some form of useful energy recovery can be invented. There is a strong incentive for a clever invention in this area.

Table 7. rf energy and AC power needs for several examples of 1 TeV linacs as compared with the 50 GeV SLC.

	SLC	Examples of 1 TeV Linacs		
Frequency (MHz)	2856	2856	2856	2856 × 5
r/Q (ohms/m)	4100	5000	5000	25000
V (GeV)	50	1000	1000	1000
E (MV/m)	20	20	100	100
L (km)	3	50	10	10
WL (kJ)	13.6	223	1117	44.7
Average P_{rf} at 180 pps (MW)	2.5	40	201	8
Global conversion efficiency from AC power to energy stored/sec	6.5%	25%	25%	25%
AC power/linac (MW)	38	160	804	32

The second question has to do with the energy spread of the electrons within an individual bunch. This energy spread is due to the longitudinal wake fields left behind in the linac by early electrons in a bunch which affect the energy of later ones. A discussion of this topic can be found in ref. 1, pages 17 and 117. As shown, it is possible to compensate partially for this effect by placing the bunch ahead of the crest (in space), thereby letting the rising sinusoidal field compensate for the decreased energy due to the wake fields.

In the design of the SLC, it was found that a Gaussian bunch with a σ_z of 4° centered roughly 13° ahead of crest had close to 85% of its charge within an energy spread of 1%. A recent study[15] has shown that this energy spread can be reduced essentially to zero by properly shaping the bunch and placing it at the correct position on the rf wave. Although some of the bunch shapes that have this property may be difficult to generate with a damping ring, it appears that a truncated Gaussian bunch can approximate the ideal bunch very closely. Thus for example, for the SLC, a Gaussian bunch ($5 \times 10^{10}\,e$) with a σ_z of 8.3° truncated at ±7.5° and centered 6.5° ahead of crest results in a total energy spread of 0.26%. The energy decrease from riding off-crest is only 3% or 1.5 GeV. Such a bunch shape might be obtained by clipping the wings of the Gaussian with energy slits in the RTL line downstream of the compressor (fig. 3). It is believed that this result can be generalized within certain limits of charge to any linear collider if the gradient and wakefield are known.

The third question has to do with the ultimate accelerating gradients which can be attained in periodic structures with metal boundaries. Indeed, very little information has been available on whether the gradients of 100 MV/m shown in table 7 can actually be realized. A short section (<1 m) of the SLAC disk-loaded structure was tested in a resonant ring in the early 1960s and incomplete documentation on this test indicated that the accelerating gradient reached 46 MV/m before the ring actually ran out of drive power. For this reason, a new study was recently started at SLAC[16] to push these measurements further. It turns out that to obtain an accelerating gradient of 100 MV/m in a SLAC three-meter section would necessitate a 900 MW klystron which is obviously not available at this time. For this reason, the tests that are presently being conducted make use of a short (seven cavities) standing-wave section ($2\pi/3$ phase shift per cavity at 2856 MHz) which is driven by a 36 MW klystron with a 2.5 μsec pulse width. As this paper is being written, extremely encouraging results have already been obtained in that the equivalent traveling-wave accelerating field has reached 130 MV/m without breakdown. The corresponding maximum peak field at the disk edge is 260 MV/m. Considerably more work in this area at this and other frequencies of interest is of course needed to draw some general conclusions. It will also have to be seen whether better shaping of the cavities can further improve both their rf and breakdown characteristics. A large body of very interesting work lies ahead.

Acknowledgements

The work reported in this paper is the result of a large collective effort by a substantial fraction of the SLAC technical staff. The author wishes to thank J. Clendenin, J. Sheppard, R. Miller, H. Schwarz, A. Millich, S. Ecklund, J. Seeman, D. Farkas, R. Stiening, A. Hutton, D. Getz and Juwen Wang who were helpful in supplying information and material for this report.

References

1. SLAC Linear Collider, Conceptual Design Report, SLAC-229.
2. B. Richter *et al.*, Proc. XIth Int. Conf. on High Energy Accelerators, Geneva (1980), p. 168.
3. H. Wiedemann, IEEE Transactions on Nuclear Science, **NS-28**, No. 3, June 1981.
4. M. B. James *et al.*, IEEE Transactions on Nuclear Science, **NS-30**, No. 4, August 1983.
5. J. E. Clendenin *et al.*, Making Electron Beams for the SLC Linac, 1984 Linear Accelerator Conference, Seeheim/Darmstadt, West Germany, May 1984.
6. J. C. Sheppard *et al.*, Acceleration of High Charge Density Electron Beams in the SLAC Linac, 1984 Linear Accelerator Conference, Seeheim/Darmstadt, West Germany, May 1984.
7. 1984 Stanford Linear Collider Handbook, Chapter 5.
8. S. D. Ecklund, private communication.
9. Z. Farkas *et al.*, IEEE Transactions Nuclear Science, **NS-22**, No. 3, 1299 (1975).
10. G. T. Konrad, High Power rf Klystrons for Linear Accelerators, 1984 Linear Accelerator Conference, Seeheim/Darmstadt, West Germany, May 1984.
11. J. D. Fox and H. D. Schwarz, IEEE Trans. Nucl. Sci. **NS-30**, No. 4, 2264 (1983).
12. M. C. Crowley-Milling, Trends in Accelerator Control Systems, 1984 Linear Accelerator Conference, Seeheim/Darmstadt, West Germany, May 1984.
13. R. Melen, IEEE Transactions on Nuclear Science **NS-28**, No. 3, June 1981.
14. R. B. Neal, Accelerator Parameters for an e^+e^- Super Linear Collider, SLAC/AP-7, September 1983.
15. Juwen Wang and G. A. Loew, Minimizing the Energy Spread Within a Single Bunch by Shaping Its Charge Distribution, SLAC/AP-25, June 1984.
16. Juwen Wang and G. A. Loew, Measurements of Ultimate Accelerating Gradients in the SLAC Disk-Loaded Structure, SLAC/AP-26, June 1984.